

**Chemical changes demonstrated in
cartilage by synchrotron infrared
microspectroscopy in an antibody-induced
murine model of rheumatoid arthritis**

Allyson M. Croxford
Kutty Selva Nandakumar
Rikard Holmdahl
Mark J. Tobin
Don McNaughton
Merrill J. Rowley

Chemical changes demonstrated in cartilage by synchrotron infrared microspectroscopy in an antibody-induced murine model of rheumatoid arthritis

Allyson M. Croxford,^{a,b} Kutty Selva Nandakumar,^c Rikard Holmdahl,^c Mark J. Tobin,^d Don McNaughton,^b and Merrill J. Rowley^a

^aMonash University, Department of Biochemistry and Molecular Biology, Clayton, Victoria, Australia

^bMonash University, Centre for Biospectroscopy and School of Chemistry, Clayton, Victoria, Australia

^cKarolinska Institute, Medical Inflammation Research, MBB, Stockholm, Sweden

^dAustralian Synchrotron, Clayton, Victoria, Australia

Abstract. Collagen antibody-induced arthritis develops in mice following passive transfer of monoclonal antibodies (mAbs) to type II collagen (CII) and is attributed to effects of proinflammatory immune complexes, but transferred mAbs may react directly and damagingly with CII. To determine whether such mAbs cause cartilage damage *in vivo* in the absence of inflammation, mice lacking complement factor 5 that do not develop joint inflammation were injected intravenously with two arthritogenic mAbs to CII, M2139 and CIIC1. Paws were collected at day 3, decalcified, paraffin embedded, and 5- μm sections were examined using standard histology and synchrotron Fourier-transform infrared microspectroscopy (FTIRM). None of the mice injected with mAb showed visual or histological evidence of inflammation but there were histological changes in the articular cartilage including loss of proteoglycan and altered chondrocyte morphology. Findings using FTIRM at high lateral resolution revealed loss of collagen and the appearance of a new peak at 1635 cm^{-1} at the surface of the cartilage interpreted as cellular activation. Thus, we demonstrate the utility of synchrotron FTIRM for examining chemical changes in diseased cartilage at the microscopic level and establish that arthritogenic mAbs to CII do cause cartilage damage *in vivo* in the absence of inflammation. © 2011 Society of Photo-Optical Instrumentation Engineers (SPIE). [DOI: 10.1117/1.3585680]

Keywords: synchrotron Fourier-transform infrared microspectroscopy; cartilage; monoclonal antibodies; collagen antibody-induced arthritis; type II collagen.

Paper 10568RR received Oct. 21, 2010; revised manuscript received Mar. 29, 2011; accepted for publication Apr. 11, 2011; published online Jun. 1, 2011.

1 Introduction

Collagen-induced arthritis (CIA) is an animal model of human rheumatoid arthritis (RA) induced by immunization with type II collagen (CII), the most abundant protein in the cartilage.^{1–4} Autoantibodies to CII occur in both CIA and RA, and intravenous injection of particular monoclonal antibodies (mAbs) to CII can induce arthritis in naïve mice.^{5–8} This passively transferred collagen antibody-induced arthritis (CAIA) develops within two to four days, depending on the genetic background of the mice, although a further injection of lipopolysaccharide may be required for enhanced incidence and severity. Mice injected with the mAbs develop swollen joints with an influx of inflammatory and synovial cells into the joint cavity, and accompanying cartilage degradation. It is a highly efficient model of inflammatory arthritis that is used widely, commercially, to assess the efficiency of potential anti-inflammatory drugs.

CAIA is generally considered to result from an inflammatory response to immune complexes of antibody and CII formed on the surface of the joint as mice that are unable to develop an inflammatory response do not develop macroscopic arthritis, and the cartilage degradation has been attributed to the action of

degradative enzymes released by the inflammatory cells. However, we have previously shown using *in vitro* systems based on cartilage explants, that two mAbs to CII, M2139 and CIIC1, which are arthritogenic *in vivo*^{7,8} adversely affect the cartilage matrix integrity and cause changes to the chemical structure of the cartilage as measured by Fourier-transform infrared microspectroscopy (FTIRM), including loss of proteoglycans, and progressive denaturation and loss of collagen from the surface where the antibodies penetrated.⁹ These changes occurred *in vitro* in the absence of any inflammatory cells, but their significance *in vivo* remained unclear.

Articular cartilage is an avascular tissue that consists of sparsely located individual chondrocytes in an abundant extracellular matrix (ECM), which represents ~95% of the cartilage tissue volume.¹⁰ The ECM comprises a network of collagen fibers, mainly CII, in which are enmeshed a variety of sulphated glycoproteins, particularly aggrecan and the unsulphated glycosaminoglycan hyaluronan.^{10,11} Collagen, primarily CII, comprises approximately 10–20% of the wet weight of the cartilage¹⁰ and provides the tensile strength of the cartilage matrix.^{10,12} These interactions are essential for the structural stability of cartilage, and we postulate that arthritogenic mAbs cause cartilage damage by binding specifically to critical structural regions on collagen fibrils that are sites of interaction between CII and matrix components or chondrocytes. If so, such

Address all correspondence to: Merrill J Rowley, Department of Biochemistry and Molecular Biology, Monash University, Wellington Road, Clayton Vic 3800 Australia. Tel: +61 3 9905 1438; Fax: +61 3 9905 3726; E-mail: Merrill.Rowley@monash.edu.

damage should be also detectable *in vivo*, in the absence of inflammation.

In the present study, we examined whether the mAbs M2139 and CIIC1 cause direct damage *in vivo* to the cartilage matrix in the absence of any inflammation, following injection of mice that lack complement factor C5, and hence are resistant to the development of inflammatory arthritis with these mAbs. Because of a lack of other appropriate biochemical or histological techniques, synchrotron FTIR-microspectroscopy was used to provide the lateral resolution necessary to examine changes to the cartilage matrix and cells in the small distal interphalangeal joints in the presence of mAbs without any prior knowledge of the chemical changes occurring.

2 Materials and Methods

2.1 Monoclonal Antibodies

The mAbs used were derived from hybridomas developed from CII-immunized mice as described previously.⁸ Briefly, hybridomas were cultured in CL-1000 flasks (Integra Biosciences, Wallisellen, Switzerland) using Dulbecco's Glutamax-I medium containing ultralow bovine IgG (Gibco BRL, Invitrogen AB, Stockholm, Sweden). Antibodies were purified using γ -Bind Plus affinity gel matrix (GE Healthcare Bio-Sciences AB, Uppsala, Sweden). The IgG content was determined from the weight of freeze-dried preparations. The antibody solutions were sterile filtered and stored at -80°C until used. M2139 and CIIC1 are arthritogenic mAbs that bind to separate well-defined conformational epitopes within the helical region of the collagen molecule, at the J1 epitope, amino acids 551–564 for M2139 and the C1¹ epitope, amino acids 359–363 for CIIC1.

2.2 Injection of Arthritogenic mAbs into Mice

To determine whether the arthritogenic mAbs cause cartilage damage *in vivo* in the absence of inflammation, paws were examined from mice three days after intravenous injection with a mixture of the two mAbs, M2139 and CIIC1 in phosphate-buffered saline (PBS) pH 7.4. Four mice from two strains were used: B10.Q mice that develop CAIA but require a further injection of lipopolysaccharide for enhanced incidence and severity of arthritis⁷ and B10.Q C5-congenic mice that lack complement factor C5 (C5 δ) and hence do not develop CAIA.¹³ C5 δ congenic mice were generated using the speed congenic technique.¹⁴ The congenic fragment from non-obese diabetic mice (NOD) in the B10.Q genetic background was ~ 54 Mb, ranging from D2Mit116 to D2Mit91. None of the mice used in this study developed macroscopic arthritis by day 3. The mixture of M2139 and CIIC1 contained 4.5 mg of each of the sterile-filtered antibody solutions in a final volume of 0.4 ml. Mice of the same strains injected with PBS alone were used as controls. Mice were killed at day 3 after injection, and paws were fixed in 4% phosphate-buffered paraformaldehyde solution for 24 h, decalcified for three to four weeks in an ethylenediaminetetraacetic acid-polyvinylpyrrolidone-Tris solution (pH 6.9), dehydrated, and embedded in paraffin using standard protocols for processing for histology and for synchrotron FTIRM.

2.3 Examination of the Cartilage

2.3.1 Histology

To examine the cartilage in the small joints, the paws of the mice were sectioned to a depth that allowed examination of both the bone and the cartilage surface within the joints. Then, 5- μm sections were stained with haematoxylin and eosin (H&E) to examine the appearance and integrity of the cartilage and chondrocytes, or with toluidine blue to examine proteoglycan loss. The thickness of the cartilage in various joints was measured using MCIDTM Image Analysis Software (M4 3.0 Rev 1.1, Imaging Research Inc., St. Catharines, Ontario, Canada). Images were captured at 200 \times magnification on H&E stained sections, and the autoselect tool was used to designate and create a line at the bone-cartilage junction. Using the two-point straight-line measurement tool, the distance of loss was measured from the edge of the tissue, through to the line created by the autoselect tool. The measurement was performed six times on each image captured.

2.3.2 Fourier-transform infrared microscopy

For examination by synchrotron FTIRM, 5- μm sections of paraffin-embedded tissue were placed onto MirrIR low-e microscope slides (Kevley Technologies, Chesterland, Ohio). To obtain the requisite resolution, measurements were performed on the IR beamline at the Australian Synchrotron (Melbourne, Victoria, Australia). Spectra were collected with a Bruker Hyperion 2000 IR microscope (Bruker Optik GmbH, Ettlingen, Germany) equipped with a liquid-nitrogen-cooled narrowband HgCdTe (MCT) detector with a 36 \times (0.5 NA) IR objective. The Hyperion 2000 microscope is coupled to a Bruker Vertex 80 spectrometer. For FTIR mapping and single-point measurements, the aperture was set at 5 \times 5 μm . For each sample examined, single-point measurements and spectral maps (grids) were collected in transmittance mode by scanning the computer-controlled microscope stage in a raster pattern with a 5- μm step size in both the x and y directions for the maps.

Because the mAbs bind to the cartilage surface^{8,15,16} for each joint examined, 10 single-point spectra were collected from chondrocytes close to the cartilage surface and 10 spectra were collected from the cartilage matrix between the cells at the surface. Similarly, 10 spectra were collected from chondrocytes and the cartilage matrix deeper within the cartilage, to compare changes associated with direct mAb penetration at the cartilage surface and changes beyond the area of direct mAb penetration. Single-point spectra were examined using OPUS 6.5 spectroscopic software (Bruker, Germany), where second-derivative spectra were used to enable the spectral resolution of bands that contribute to either inflection points or shoulders in the original spectrum¹⁷ while also greatly reducing the contribution of sloping baselines observed in some absorbance spectra.

Grids were defined over the distal interphalangeal joints that encompassed regions of the cartilage surface and included the bone beyond the cartilage surface. The spectra obtained from the grids were analyzed using CytoSpec (CytoSpec, Inc., Berlin, Germany), performing unsupervised hierarchical cluster analysis (UHCA)¹⁸ to generate false color maps based on spectral variation. UHCA is a multivariate approach to analyzing a data set of spectra collected from tissue by FTIRM and has been well

described in literature.^{18–20} It provides an objective means for determining variations in the tissue without any prior knowledge of changes that may be occurring. A “quality test” was performed to remove spectra with poor signal-to-noise ratios and spectra of very high or low absorbance and analysis was directed toward the spectral region $940\text{--}1800\text{ cm}^{-1}$, where the major macromolecular spectral bands appear. Spectra at the tissue periphery that showed dispersion effects and hence confound analysis of the amide bands were also removed.

Because the major components of the cartilage matrix are collagen, sulphated proteoglycans, and the nonsulphated glycosaminoglycan hyaluronan, analysis was directed particularly to the location of the amide I peak ($1640\text{--}1670\text{ cm}^{-1}$), representing total protein and to peaks within the region of $960\text{--}1175\text{ cm}^{-1}$ derived from carbohydrate moieties.⁹ The amide I peak for native triple helical collagen is unusual, being $>1660\text{ cm}^{-1}$, compared to most other proteins for which the peak is $\sim 1650\text{ cm}^{-1}$, and there is a characteristic shift to lower wavenumber on denaturation.^{21–24} The “collagen triplet” of peaks at 1203 , 1234 , and 1280 cm^{-1} often used to identify collagen in other tissues is of limited utility in the analysis of cartilage, as it overlaps the peak at $1240\text{--}1245\text{ cm}^{-1}$ derived from sulphates,^{22,25} which are a major component of the highly sulphated glycosaminoglycans of the cartilage matrix. For the analysis of chondrocytes, particular attention was paid to bands in the second-derivative spectra that could be attributed to nuclear deoxyribose nucleic acid (DNA), or ribonucleic acid (RNA), which may be increased in activated cells. These include bands at 1240 and 1080 cm^{-1} attributed to the asymmetric and symmetric phosphate stretching vibrations ($\nu_{\text{as}}\text{PO}_2^-$ and $\nu_{\text{s}}\text{PO}_2^-$) of cellular nucleic acids, bands at 1050 and 1015 cm^{-1} characteristic of ribose sugars, and a band at 970 cm^{-1} , characteristic of phosphodiester main chain vibrations.¹⁷ An important component of this study was the need for optimum lateral resolution and careful comparison of the visual images to localize the IR spectra obtained, to examine the chondrocytes, and to discriminate the cartilage from bone, noting that the major protein in decalcified bone is type I collagen, which has an almost identical IR spectrum to that of the type II collagen in cartilage.

3 Results

3.1 Histology of Joints

Sections of paws from mice treated with mAbs and from control mice were examined by light microscopy. Whereas the cartilage surface in the joints of control mice was smooth, shown by H&E staining [Fig. 1(a)] and the proteoglycans stained strongly with toluidine blue [Fig. 1(c)], the cartilage of mice of both strains treated with the mAbs showed considerable variability in appearance [Fig. 1(b) and 1(d)]. Unlike the cartilage surface in the control mice, the cartilage surface in the mice treated with mAbs was often uneven, with cells protruding from the cartilage surface [Fig. 1(b)]. There was a dramatic reduction in the intensity of staining of proteoglycans in the majority of joints, particularly in the small distal interphalangeal joints where there were cells protruding from the cartilage surface and dark “ringing” of stain around the cells suggestive of new proteoglycan synthesis [Fig. 1(d)]. By MCID analysis of 17 distal interphalangeal joints from six mice of the two strains

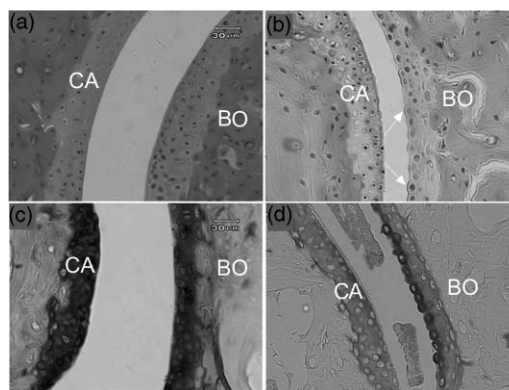


Fig. 1 Histological sections through joints from control and mAb-treated mice showing the cartilage: (a) Control joint stained with H&E, showing a smooth cartilage surface; (b) joint from mAb-treated mouse stained with H&E, showing an uneven cartilage surface, due to cells protruding from the cartilage surface; (c) control joint stained with toluidine blue to show dark, uniform staining of proteoglycans; and (d) joint from mAb-treated mouse stained with toluidine blue, showing loss of proteoglycan staining and dark “ringing” of stain around protruding surface chondrocytes. All images in this figure are on the same scale. CA: cartilage, BO: bone, arrows indicate protruding chondrocytes.

treated with mAb, the cartilage that showed these “protruding” cells was significantly thinner than cartilage from joints in which the surface remained smooth (mean \pm standard deviation, 33 ± 7 versus $49 \pm 6\ \mu\text{m}$, $p = 0.004$), suggesting that there was loss of matrix from the cartilage surface. The changes following mAb injection were similar in both strains of mice tested.

3.2 Synchrotron FTIRM Analysis of the Cartilage: Comparison of Chondrocytes and Matrix

Single-point spectra of the cartilage matrix were compared from interphalangeal joints from mAb-treated mice and from control mice. For both groups, the averaged absorbance spectra after baseline correction were very similar and characteristic of cartilage [Fig. 2(a)], but the groups differed in two characteristics. First, there was a substantial decrease in absorbance in peaks of $<1500\text{ cm}^{-1}$, including the peak at $1240\text{--}1245\text{ cm}^{-1}$ derived from sulphates and peaks within the region $960\text{--}1175\text{ cm}^{-1}$ derived from carbohydrate moieties; these changes were consistent with the loss of proteoglycans shown by histological staining in treated mice. Second, there was a shift in location of the amide I peak, from 1670 to 1656 cm^{-1} in the mAb-treated mice, taken to represent collagen denaturation. Spectra from the chondrocytes were very similar to those from the matrix in both groups, and no peaks could be identified that occurred only in the chondrocytes.

Individual spectra were further analyzed using second-derivative analysis to assign bands. Overall, spectra from both chondrocytes and matrix were very similar and the proteoglycan loss identified by toluidine blue staining and seen in the underivatized spectra was not apparent using second-derivative spectra, suggesting that the proteoglycan loss was not associated with any major changes in those components. Moreover, second-derivative spectra from the chondrocytes did not show any bands that could be unequivocally assigned to nucleic acid bands of either DNA or RNA.

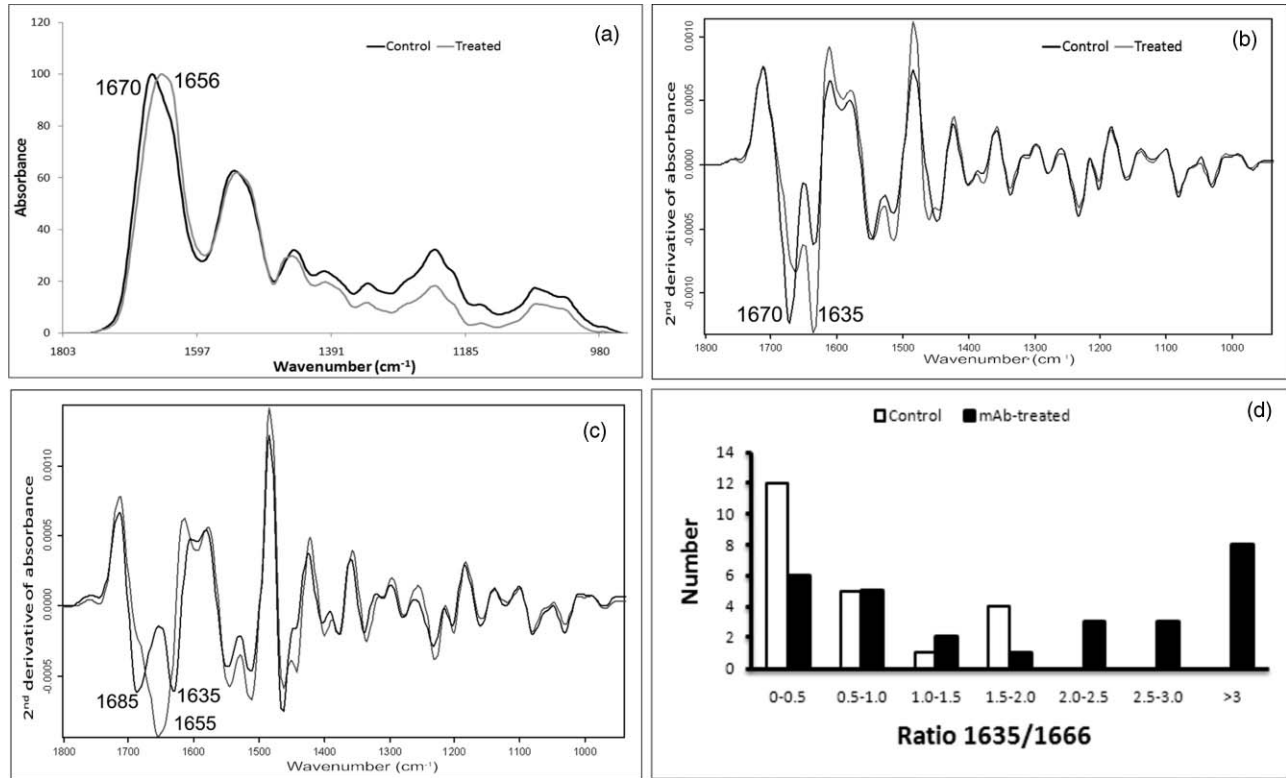


Fig. 2 Patterns of spectra from control and mAb-treated mice: (a) Mean absorbance spectra from matrix from control mice and a mAb-treated mouse after background correction and normalization based on the Amide I peak; (b) mean second-derivative spectra from the same mice, showing the most frequently seen pattern with two bands at 1666–1670 cm^{-1} and at 1635–1637 cm^{-1} ; (c) uncommon patterns of second-derivative spectra, a single peak at 1655 cm^{-1} corresponding to an underivatized absorbance peak in the same position (light gray) or two peaks with a marked shift of one to 1685 cm^{-1} (black); and (d) differing distribution of spectra of control mice and mAb-treated mice according to ratios 1635/1666 calculated based on the value of the minima in second-derivative spectra.

The major differences in the second-derivative spectra were in the amide I region, $>1600 \text{ cm}^{-1}$. In $>90\%$ of all spectra, two bands were identified as components of the amide I peak, one in the region of 1660–1670 cm^{-1} and a second at 1635–1637 cm^{-1} [Fig. 2(b)]. The band at 1635–1637 cm^{-1} could be identified as a shoulder on the amide I peak in the underivatized spectrum, and an increase in its intensity when compared to the 1660–1670 cm^{-1} band, which corresponded to a shift in the amide I peak to a lower wavenumber in the original spectrum. This pattern was seen in $>90\%$ of all individual spectra from either matrix or chondrocytes, and either control or mAb-treated mice, but there were differences in the relative intensity of the two bands according to the source of the spectrum.

Two further patterns of bands in the amide I region also occurred infrequently [Fig. 2(c)]. In one, the band at 1660–1670 cm^{-1} was replaced by a band at 1680–1685 cm^{-1} , often with a small band at 1635–1637 cm^{-1} . In the other, there was a band around 1654 cm^{-1} , usually alone, but sometimes associated with bands at 1666–1670 and/or 1635 cm^{-1} , and seen as an amide I peak in the underivatized spectrum at $\sim 1655 \text{ cm}^{-1}$. This pattern was rare in the mouse spectra but corresponded to spectra we have attributed to collagen denaturation in cartilage explants treated with the mAbs *in vitro*.^{9,26} These two patterns of bands occurred too rarely for analysis, but may provide information about the secondary structure of the collagen matrix

(see Sec. 4). In a preliminary experiment, a ratio 1635/1666 was calculated from the value of minima in the second-derivative spectra at each wavenumber for 22 surface-located cells from control mice and 28 cells from mAb-treated mice [Fig. 2(d)]. The mean ratio 1635/1666 for the control cells was 0.65 (range 0–2), which was significantly lower than 3.4 (range 0.12–11) for the mAb-treated cells ($p < 0.001$, Mann-Whitney U test). Overall, only 5 of the 22 second-derivative spectra from control mice showed a ratio 1635/1666 > 1 , compared to 19 of 28 of the spectra from mAb-treated mice ($p = 0.0015$, χ^2). Because ratios > 1 were readily identified from individual second-derivative spectra, in all further analysis results have been expressed as the number in each group > 1 .

Table 1 and Fig. 3 show the results of analysis of cells or matrix that showed the common pattern of reactivity in controls and mAb-treated mice. For the control mice, the spectra differed little between the surface and deep in the cartilage [Fig. 3(a) and 3(c)]. The spectra from the mAb-treated mice were more variable, and there were differences between the spectra derived at the cartilage surface and deep within the cartilage, particularly for the chondrocytes [Fig. 3(b) and 3(d)]. The major spectral changes in the treated mice were seen in the amide I region, $>1600 \text{ cm}^{-1}$; although in all cases, loss of peak height was clearly apparent in the nonderivatized spectra (data not shown). At or near the cartilage surface, the band at 1635 cm^{-1} was prominent in all spectra and, for the chondrocytes, this band

Table 1 Relative prominence of second-derivative bands in the amide 1 region at 1635 and 1666 cm^{-1} for cells and matrix from mAb-treated and control mice.

| | mAb-treated (n = 8 mice) | Control (n = 3 mice) | p (χ^2) |
|-------------------------|--------------------------|----------------------|----------------|
| Surface cells | | | |
| Spectra examined | 106 | 30 | |
| Ratio > 1 | 57 (54%) ¹ | 9 (30%) | 0.0214 |
| Mean ratio ² | 1.3 | 0.55 | |
| Surface matrix | | | |
| Spectra examined | 69 | 30 | |
| Ratio > 1 | 24 (35%) | 4 (13%) | 0.0199 |
| Mean ratio | 1.7 | 0.32 | |
| Deep cells | | | |
| Spectra examined | 80 | 30 | |
| Ratio > 1 | 8 ³ (10%) | 0 (0%) | ns |
| Mean ratio | 1.7 | 0.13 | |
| Deep matrix | | | |
| Spectra examined | 80 | 30 | |
| Ratio > 1 | 0 (0%) | 0 (0%) | ns |
| Mean ratio | 0.02 | 0.04 | |

1. Number (%) of individual spectra in which 1635 cm^{-1} was the major band (ratio > 1).
 2. Ratio 1635/1666 based on the value of the minima in the mean second-derivative spectrum.
 3. From a single mouse.
- ns: Not significant.

was often stronger than the band at 1666 cm^{-1} (Table 1). Thus, for 106 surface chondrocytes examined from eight mAb-treated mice, the mean ratio 1635/1666 bands for the treated mice was 1.25 (range 0.36–3.3), compared to 0.55 (range 0.08–1.2) for 28

chondrocytes from three control mice, and the 1635 cm^{-1} was the major band in significantly more of the mAb-treated mice (57/106, 54% versus 9/30, 30% $p = 0.0214$, χ^2). Deeper in the cartilage, the spectra for both chondrocytes and matrix were similar to those of controls and, the band at 1635 cm^{-1} seen at the surface, was noticeably reduced (mean ratio 1635/1666, 0.038, range 0.038–0.068).

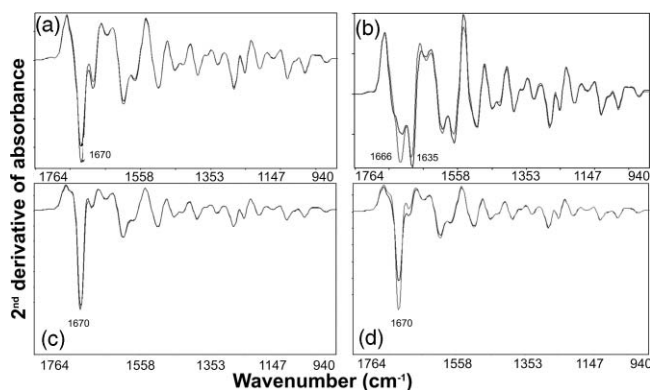


Fig. 3 Representative single point synchrotron FTIRM spectra collected from control and mAb-treated mice, comparing the spectra obtained from the chondrocytes and from the cartilage matrix at the edge of the cartilage (a,b) and deeper in the cartilage (c,d). The bold line represents the chondrocytes and the pale line indicates cartilage matrix. (a) Spectra at the cartilage surface in a control mouse, (b) spectra at the cartilage surface in an mAb-treated mouse, (c) spectra deeper in the cartilage in a control mouse, and (d) spectra deeper in the cartilage in an mAb-treated mouse.

3.3 Unsupervised Hierarchical Cluster Analysis of the Cartilage

Spectral maps spanning from the cartilage surface through to the bone in the distal interphalangeal joints were collected and examined using UHCA on either standard spectra or second-derivative spectra. Despite using varying numbers of clusters and performing a quality test to eliminate poor quality spectra, UHCA did not clearly distinguish between the bone and the cartilage, and spectra collected from control mice were very similar across the entire grid (Fig. 4), noting that the characteristic bands representing mineralization of the bone have been removed by decalcification. The major amide I band in each cluster was located above 1660 cm^{-1} , characteristic of collagen, whether the type II collagen in the cartilage, or the type I collagen of bone, and there were bands at 1203, 1234, and 1280 cm^{-1} that could be ascribed to the “collagen triplet.” In several joints from the control mice, cluster analysis discriminated a cluster

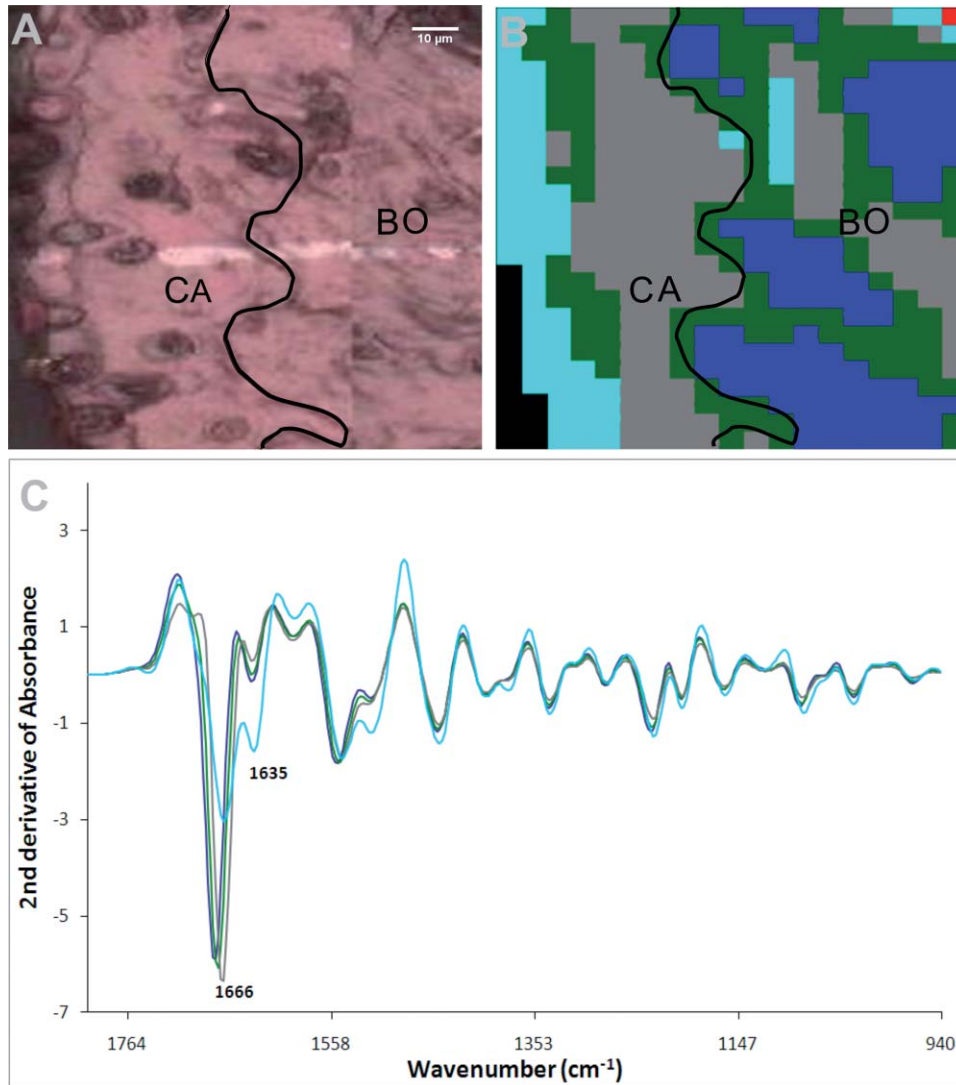


Fig. 4 Representative result obtained by synchrotron FTIRM on a grid from a control mouse. (a) Light microscopy image of unstained section on Kevley reflective slide. CA: cartilage, BO: bone, \blackline cartilage border. (b) IR image processed by UHCA over the range 940–1800 cm^{-1} using second-derivative spectra with five clusters. (c) Second-derivative spectra for the clusters, corresponding to the image in (b), showing a band at 1635 cm^{-1} in the cluster corresponding to the cartilage surface (1635/1666 ratio 0.5, based on peak height). Pixels of poor quality were excluded from analysis. Original magnification of (a) and (b) are $\times 200$.

localized to a surface layer of the cartilage that contained a relatively high proportion of chondrocytes in which the amide I band at 1666 cm^{-1} was reduced and the minor band at 1635 cm^{-1} was prominent (Fig. 4).

The grids collected from the mice treated with mAbs were more complex. Overall spectra showed more “noise” at the cartilage surface, leading to loss of pixels, when quality tested for UHCA, and clusters at the cartilage surface were often uninformative. Figure 5 shows the results obtained from a representative mouse paw. In this sample, close to the surface, the amide I band at 1666 cm^{-1} was markedly reduced and considerably smaller than the band at 1635 cm^{-1} .

4 Discussion

This study examined the histological and chemical changes by synchrotron FTIRM in the cartilage of paws from mice injected

with two mAbs to CII, M2139, and CIIC1, which can induce arthritis.^{7,27} Until day 3, when samples were collected, none of the mice transferred with mAb showed macroscopic joint swelling or histological evidence of any infiltrating inflammatory cells. Nonetheless, there was clear histological damage to the cartilage, including proteoglycan loss and cartilage thinning in the small joints, and matrix changes identified by synchrotron FTIRM that included loss of the 1660 cm^{-1} amide I band characteristic of native CII and the appearance of an unidentified band at 1635 cm^{-1} in both the complement factor C5 sufficient and deficient mice. These results provide clear evidence that the mAbs that cause the cartilage damage *in vitro*^{9,26} also have damaging effects on the cartilage *in vivo* in the absence of inflammation.

In contrast to our previous studies using the cartilage explants *in vitro*^{9,26} in which the shift in the position of the amide I band to below 1660 cm^{-1} in absorbance spectra was accompanied

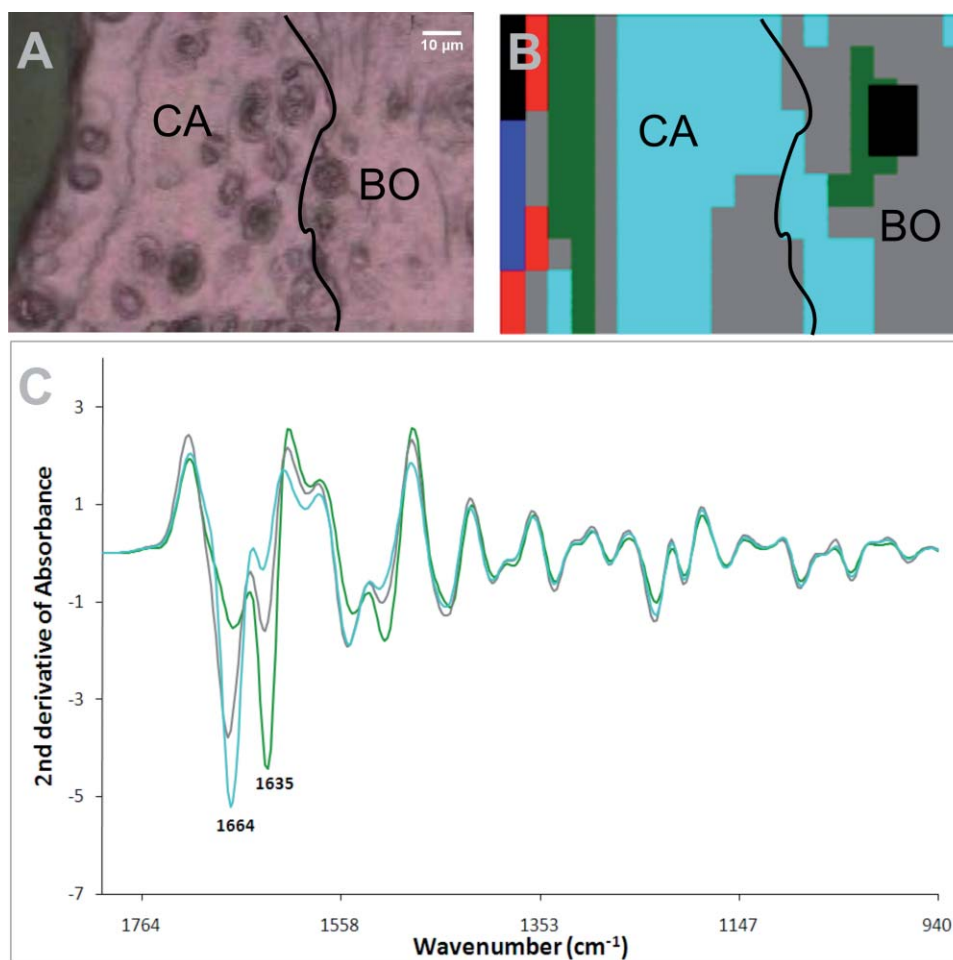


Fig. 5 Representative result obtained by synchrotron FTIRM on a grid from a mouse injected with two mAb. (a) Light microscopy image of unstained section on Kevley reflective slide CA: cartilage, BO: bone, \curvearrowright cartilage border. (b) IR image processed by UHCA over the range $940\text{--}1800\text{ cm}^{-1}$ using second-derivative spectra with five clusters. (c) Second-derivative spectra for the clusters, corresponding to the image in (b). Pixels of poor quality were excluded from analysis. At the cartilage surface the band at 1635 cm^{-1} was more prominent than the band at 1664 cm^{-1} (1635/1664 ratio 3.1). Original magnification of (a) and (b) are $\times 200$.

by a similar shift in second-derivative spectra in the cartilage cultured with mAbs, this shift representative of collagen denaturation was much less prominent *in vivo*. Instead, there was evidence of complete loss of collagen, seen as a decrease in the strength of the amide I band, particularly at the cartilage surface, and measurable thinning of the cartilage. This may represent differences in the processing of denatured collagen in the tissue *in vivo* and *in vitro*. Although native collagen is highly resistant to degradation by proteases other than collagenases, denatured collagen is readily degraded by a variety of enzymes. *In vivo*, denatured collagen would be rapidly removed by various matrix metalloproteinases (MMPs) not only by the gelatinases MMP-2 and 9,²⁸ but also by MMP-3 (stromelysin-1), which by degrading the pericellular extracellular matrix components further activates the cartilage-degrading enzymes such as proMMP-1, proMMP-9, and proMMP-13²⁹ with the result that there is complete loss of matrix. By contrast, *in vitro*, these enzymes may be less abundant, leading to less rapid removal of the denatured collagen and, hence, its appearance in spectra.

Despite the use of the high lateral resolution of the synchrotron to examine the spectra of the chondrocytes, the spectra obtained from both the chondrocytes and matrix were very sim-

ilar. The abundance of the ECM means that the IR spectrum of cartilage primarily represents its major components, particularly CII, with little contribution from cellular components such as DNA, RNA, or other proteins. Because chondrocytes are the cells that synthesize, assemble, and secrete the components of the ECM,¹² these components are likely to contribute to the cellular spectra also.

A major difference from previous *in vitro* studies was the appearance of a band at 1635 cm^{-1} that appeared as a shoulder on the amide I band in the nonderivatized spectra. This was distinct from the shift in the amide I peak we have previously observed in the cartilage explant cultures,^{9,26} and attributed to collagen denaturation,^{30–32} and the two bands could be discriminated in second-derivative spectra. Moreover, as spectra at the tissue periphery that showed dispersion effects were removed, and a similar band was occasionally seen deep in the tissue, this distinct peak could not be explained by a shift of the amide I band resulting from scattering effects close to the edge of tissue samples, as has been reported elsewhere.³³ In some mAb-treated mice, the band at 1635 cm^{-1} was the dominant band in the spectrum at the cartilage surface. The nature of this peak is unknown, but a similar peak has been associated with

living chondrocytes in cartilage explants and may be associated with matrix regeneration.²⁶ In the mouse cartilage where the 1635-cm⁻¹ band occurred, surface chondrocytes often showed evidence of proteoglycan synthesis, seen as ringing in the toluidine blue-stained sections. In healthy cartilage, the turnover of the matrix is normally very slow and the half-life of CII in adult cartilage has been estimated to be 1000 days,¹¹ although there is some loss and repair of the ECM evidenced by turnover of proteoglycans, particularly aggrecan, at the joint surface, and this is increased following damage.^{11,34} Taken together, these results suggest that the 1635-cm⁻¹ band is a marker of activated chondrocytes in the cartilage.

Although the 1635 cm⁻¹ band was associated with regions that contain activated chondrocytes in the mouse cartilage, it has not been conclusively identified. Despite the heightened resolution obtained by use of synchrotron radiation, it appeared in both the spectra of chondrocytes and also extracellularly. The major protein of the cartilage is CII, a fibril forming collagen synthesized by chondrocytes, and comprising three α -helical polypeptide chains twisted tightly into a right-handed triple helix to form a ropelike structure stabilized by strong covalent bonds.^{10,12} The amide I peak of this collagen helix is characteristically above 1658–1660 cm⁻¹, appearing in deconvoluted or second-derivative spectra as three distinct bands at 1657–1661, 1630–37 cm⁻¹, and above 1670 cm⁻¹.^{23,31,32,35–37} These bands appear to be characteristic of a triple helix and also occur in other molecules that contain a collagen-like triple helix, including the nonfibrillar collagens that contain one or several small triple-helical domains interrupted by short nonhelical domains, and the complement component C1q that comprises a collagen-like triple helix at the N-terminus, with C-terminal globular heads.³⁸ In all these proteins, the band at 1657–61 cm⁻¹ is normally the strongest of the three. The 1635-cm⁻¹ band in the mouse cartilage could represent the 1630–37 cm⁻¹ band of the collagen triple helix, although it is unclear why it would be much stronger in the cartilage of the mAb-treated mice than in the control mice.

Alternatively, the 1635cm⁻¹ could represent the appearance of another band within the amide I region as a result of new protein synthesis. Bands below 1640 cm⁻¹ and particularly at 1637 cm⁻¹ are characteristic of β -strand secondary structures.^{39,40} Such structures may reflect marked increases in other unknown cartilage proteins, but they may also arise from collagen itself. Mature collagen fibrils are almost entirely triple helical in structure and hence are unlikely to contain significant β -strand secondary structures, but collagen precursors are synthesized with large C- and N-terminal extensions, which may contain β -sheet and β -turns. These extension propeptides are involved in the chain assembly necessary for the triple-helical formation that takes place within the cell prior to secretion and are cleaved by specific peptidases after secretion but prior to formation of fibrils in which the major structural unit is triple helical collagen.^{10,12} The fibrils of triple helical collagen are then aligned in a quarter-staggered array to form thicker fibrils and stabilized by cross-linking residues, including lysine. The IR spectrum of purified collagen derived by pepsin extraction reflects this triple helical secondary structure without any contribution from β -sheet structures, as pepsin cleavage removes any remaining nontriple-helical regions at the N- and C-terminus of the collagen but does not digest the triple helix itself.³⁸ However, in this study, the band at 1635 cm⁻¹ may rep-

resent β -secondary structures within the globular heads of newly synthesized collagen produced by activated chondrocytes, both within the cells and also in the matrix before fibril formation occurs. A similar change in the relative intensity of second-derivative spectra has been described for C1q where there is a strong band at 1637 cm⁻¹ for the intact molecule, taken to represent β -secondary structures within the globular domains, and only a weak band at 1661 cm⁻¹, representing the relatively low proportion of triple helix, whereas for the triple helical C1q stalks remaining after removal of the globular domains by pepsin digestion. The major band was at 1655 cm⁻¹ and assigned to the triple helical structure, with only a weak band at 1636 cm⁻¹.³⁸

Finally, this study illustrates the utility of IR microspectroscopy for examining chemical changes in cartilage by providing information that can only be deduced indirectly otherwise. In the absence of other markers of cartilage damage, the combination of standard histological analysis and FTIRM analysis should provide important new information in studies of arthritis and cartilage repair. By utilizing the higher lateral resolution available for infrared microspectroscopy at the Australian synchrotron, it has been possible to look at individual cells and areas of matrix in different joints, and at different depths in the cartilage, and to discern differences that cannot be measured by any currently available biochemical or histological techniques. We have demonstrated damage to the cartilage structure and matrix by mAbs to CII directly both *in vitro*²⁶ and in the current study *in vivo* in the absence of inflammation. Autoantibodies play an essential role in the pathogenesis of CIA and most likely also in RA.^{13,41} The exact mechanism and cause for the cartilage damage and destruction seen in RA is yet to be fully elucidated. However, these same antibodies to CII are present in RA and its murine model and may explain the cartilage damage that occurs in the human disease. Furthermore, understanding the direct damage caused by antibodies on target tissues without any major inflammatory events will stimulate further research in several antibody dependent immune pathologies.

Acknowledgments

We thank Ian Mackay and Senga Whittingham for helpful discussions and editorial comments. The work was supported by grants from the National Health and Medical Research Council of Australia, the Barbara Cameron Grant, and a project grant from Arthritis Australia, the Swedish Research Council, the Swedish Strategic Science Foundation, and the European Union Grant Masterswitch (Grant No. HEALTH-F2-2008-223404). Part of this research was undertaken on the Infrared Microspectroscopy beamline at the Australian Synchrotron, Victoria, Australia.

References

1. J. S. Courtenay, M. J. Dallman, A. D. Dayan, A. Martin, and B. Mosedale, "Immunisation against heterologous type II collagen induces arthritis in mice," *Nature* **283**, 666–668 (1980).
2. R. Holmdahl, M. Andersson, T. J. Goldschmidt, K. Gustafsson, L. Jansson, and J. A. Mo, "Type II collagen autoimmunity in animals and provocations leading to arthritis," *Immunol. Rev.* **118**, 193–232 (1990).
3. C. Steffen, "Consideration of pathogenesis of rheumatoid arthritis as collagen autoimmunity," *Z. Immunitätsforsch. Allerg. Klin. Immunol.* **139**, 219–227 (1970).

4. D. E. Trentham, A. S. Townes, and A. H. Kang, "Autoimmunity to type II collagen an experimental model of arthritis," *J. Exp. Med.* **146**, 857–868 (1977).
5. K. Terato, K. A. Hasty, R. A. Reife, M. A. Cremer, A. H. Kang, and J. M. Stuart, "Induction of arthritis with monoclonal antibodies to collagen," *J. Immunol.* **148**, 2103–2108 (1992).
6. K. S. Nandakumar and R. Holmdahl, "Antibody-induced arthritis: disease mechanisms and genes involved at the effector phase of arthritis," *Arthritis Res. Ther.* **8**, 223–233 (2006).
7. K. S. Nandakumar, L. Svensson, and R. Holmdahl, "Collagen type II-specific monoclonal antibody-induced arthritis in mice: description of the disease and the influence of age, sex, and genes," *Am. J. Pathol.* **163**, 1827–1837 (2003).
8. R. Holmdahl, K. Rubin, L. Klareskog, E. Larsson, and H. Wigzell, "Characterization of the antibody response in mice with type II collagen-induced arthritis, using monoclonal anti-type II collagen antibodies," *Arthritis Rheum.* **29**, 400–410 (1986).
9. D. E. Crombie, M. Turer, B. B. Zuasti, B. Wood, D. McNaughton, K. S. Nandakumar, R. Holmdahl, M. P. Van Damme, and M. J. Rowley, "Destructive effects of murine arthritogenic antibodies to type II collagen on cartilage explants *in vitro*," *Arthritis Res. Ther.* **7**, R927–937 (2005).
10. E. E. Coates and J. P. Fisher, "Phenotypic variations in chondrocyte subpopulations and their response to *in vitro* culture and external stimuli," *Ann. Biomed. Eng.* **38**, 3371–3388 (2010).
11. H. Muir, "The chondrocyte, architect of cartilage: biomechanics, structure, function and molecular biology of cartilage matrix macromolecules," *Bioessays* **17**, 1039–1048 (1995).
12. K. E. Kuettner, "Biochemistry of articular cartilage in health and disease," *Clin. Biochem.* **25**, 155–163 (1992).
13. K. S. Nandakumar, E. Bajtner, L. Hill, B. Bohm, M. J. Rowley, H. Burkhardt, and R. Holmdahl, "Arthritogenic antibodies specific for a major type II collagen triple-helical epitope bind and destabilize cartilage independent of inflammation," *Arthritis Rheum.* **58**, 184–196 (2008).
14. A. C. Johansson, M. Sundler, P. Kjellen, M. Johannesson, A. Cook, A. K. Lindqvist, B. Nakken, A. I. Bolstad, R. Jonsson, M. Alarcon-Riquelme, and R. Holmdahl, "Genetic control of collagen-induced arthritis in a cross with NOD and C57BL/10 mice is dependent on gene regions encoding complement factor 5 and FcγRIIb and is not associated with loci controlling diabetes," *Eur. J. Immunol.* **31**, 1847–1856 (2001).
15. R. Holmdahl, J. A. Mo, R. Jonsson, K. Karlstrom, and A. Scheynius, "Multiple epitopes on cartilage type II collagen are accessible for antibody binding *in vivo*," *Autoimmunity* **10**, 27–34 (1991).
16. J. A. Mo, A. Scheynius, S. Nilsson, and R. Holmdahl, "Germline-encoded IgG antibodies bind mouse cartilage *in vivo*: epitope- and idiotype-specific binding and inhibition," *Scand. J. Immunol.* **39**, 122–130 (1994).
17. B. R. Wood, B. Tait, and D. McNaghton, "Fourier transform infrared spectroscopy as a method for monitoring the molecular dynamics of lymphocyte activation," *Appl. Spectrosc.* **54**, 353–359 (2000).
18. P. Lasch, W. Haensch, D. Naumann, and M. Diem, "Imaging of colorectal adenocarcinoma using FT-IR microspectroscopy and cluster analysis," *Biochim. Biophys. Acta.* **1688**, 176–186 (2004).
19. M. Diem, L. Chiriboga, and H. Yee, "Infrared spectroscopy of human cells and tissue. VIII. Strategies for analysis of infrared tissue mapping data and applications to liver tissue," *Biopolymers* **57**, 282–290 (2000).
20. B. R. Wood, L. Chiriboga, H. Yee, M. A. Quinn, D. McNaughton, and M. Diem, "Fourier transform infrared (FTIR) spectral mapping of the cervical transformation zone, and dysplastic squamous epithelium," *Gynecol. Oncol.* **93**, 59–68 (2004).
21. X. Bi, G. Li, S. B. Doty, and N. P. Camacho, "A novel method for determination of collagen orientation in cartilage by Fourier transform infrared imaging spectroscopy (FT-IRIS)," *Osteoarthritis Cartilage* **13**, 1050–1058 (2005).
22. N. P. Camacho, P. West, P. A. Torzilli, and R. Mendelsohn, "FTIR microscopic imaging of collagen and proteoglycan in bovine cartilage," *Biopolymers* **62**, 1–8 (2001).
23. K. J. Payne and A. Veis, "Fourier transform IR spectroscopy of collagen and gelatin solutions: deconvolution of the amide I band for conformational studies," *Biopolymers* **27**, 1749–1760 (1988).
24. P. A. West, P. A. Torzilli, C. Chen, P. Lin, and N. P. Camacho, "Fourier transform infrared imaging spectroscopy analysis of collagenase-induced cartilage degradation," *J. Biomed. Opt.* **10**, 14015 (2005).
25. K. Potter, L. H. Kidder, I. W. Levin, E. N. Lewis, and R. G. Spencer, "Imaging of collagen and proteoglycan in cartilage sections using Fourier transform infrared spectral imaging," *Arthritis Rheum.* **44**, 846–855 (2001).
26. A. M. Croxford, D. Crombie, D. McNaughton, R. Holmdahl, K. S. Nandakumar, and M. J. Rowley, "Specific antibody protection of the extracellular cartilage matrix against collagen antibody-induced damage," *Arthritis Rheum.* **62**, 3374–3384 (2010).
27. H. Burkhardt, T. Koller, A. Engstrom, K. S. Nandakumar, J. Turnay, H. G. Kraetsch, J. R. Kalden, and R. Holmdahl, "Epitope-specific recognition of type II collagen by rheumatoid arthritis antibodies is shared with recognition by antibodies that are arthritogenic in collagen-induced arthritis in the mouse," *Arthritis Rheum.* **46**, 2339–2348 (2002).
28. C. J. Malemud, "Matrix metalloproteinases (MMPs) in health and disease: an overview," *Front. Biosci.* **11**, 1696–1701 (2006).
29. A. Kobayashi, S. Naito, H. Enomoto, T. Shiomi, T. Kimura, K. Obata, K. Inoue, and Y. Okada, "Serum levels of matrix metalloproteinase 3 (stromelysin 1) for monitoring synovitis in rheumatoid arthritis," *Arch. Pathol. Lab. Med.* **131**, 563–570 (2007).
30. R. Bhargava and I. W. Levin, "Fourier transform infrared imaging: theory and practice," *Anal. Chem.* **73**, 5157–5167 (2001).
31. A. George and A. Veis, "FTIRS in H₂O demonstrates that collagen monomers undergo a conformational transition prior to thermal self-assembly *in vitro*," *Biochemistry* **30**, 2372–2377 (1991).
32. Y. A. Lazarev, B. A. Grishkovsky, and T. B. Khromova, "Amide I band of IR spectrum and structure of collagen and related polypeptides," *Biopolymers* **24**, 1449–1478 (1985).
33. P. Bassan, A. Kohler, H. Martens, J. Lee, H. J. Byrne, P. Dumas, E. Gazi, M. Brown, N. Clarke, and P. Gardner, "Resonant Mie scattering (RMieS) correction of infrared spectra from highly scattering biological samples," *Analyst* **135**, 268–277 (2010).
34. M. A. Campbell, C. J. Handley, and S. E. D'Souza, "Turnover of proteoglycans in articular-cartilage cultures: characterization of proteoglycans released into the medium," *Biochem. J.* **259**, 21–25 (1989).
35. R. D. Fraser, T. P. MacRae, and E. Suzuki, "Chain conformation in the collagen molecule," *J. Mol. Biol.* **129**, 463–481 (1979).
36. K. Okuyama, S. Arnott, M. Takayanagi, and M. Kakudo, "Crystal and molecular structure of a collagen-like polypeptide (Pro-Pro-Gly)₁₀," *J. Mol. Biol.* **152**, 427–443 (1981).
37. C. Petitbois, G. Gousspillou, K. Wehbe, J. P. Delage, and G. Deleris, "Analysis of type I and IV collagens by FT-IR spectroscopy and imaging for a molecular investigation of skeletal muscle connective tissue," *Anal. Bioanal. Chem.* **386**, 1961–1966 (2006).
38. K. F. Smith, P. I. Haris, D. Chapman, K. B. Reid, and S. J. Perkins, "Beta-sheet secondary structure of the trimeric globular domain of C1q of complement and collagen types VIII and X by Fourier-transform infrared spectroscopy and averaged structure predictions," *Biochem. J.* **301**(Pt 1), 249–256 (1994).
39. D. M. Byler and H. Susi, "Examination of the secondary structure of proteins by deconvolved FTIR spectra," *Biopolymers* **25**, 469–487 (1986).
40. W. K. Surewicz, H. H. Mantsch, and D. Chapman, "Determination of protein secondary structure by Fourier transform infrared spectroscopy: a critical assessment," *Biochemistry* **32**, 389–394 (1993).
41. K. S. Nandakumar, "Pathogenic antibody recognition of cartilage," *Cell Tissue Res.* **339**, 213–220 (2010).